



City Research Online

City St George's, University of London

Citation: Moreno-Ramirez, C., Tomas-Rodriguez, M. & Evangelou, S. A. (2019). Effects of interconnected suspension systems on the dynamics of sport motorcycles. Paper presented at the Bicycle and Motorcycle Dynamics 2019 Symposium on the Dynamics and Control of Single Track Vehicles, 09 - 11 September 2019, University of Padova, Italy.

This is the accepted version of the paper.

This version of the publication may differ from the final published version. To cite this item please consult the publisher's version.

Permanent repository link: <https://openaccess.city.ac.uk/id/eprint/23193/>

Copyright and Reuse: Copyright and Moral Rights remain with the author(s) and/or copyright holders. Copies of full items can be used for personal research or study, educational, or not-for-profit purposes without prior permission or charge, unless otherwise indicated, provided that the authors, title and full bibliographic details are credited, a hyperlink and/or URL is given for the original metadata page and the content is not changed in any way. For full details of reuse please refer to [City Research Online policy](#).

Effects of Interconnected Suspension Systems on the In-plane Dynamics of Sport Motorcycles

C. Moreno-Ramírez*, M. Tomás-Rodríguez#, S. A. Evangelou†

* Department of Industrial Engineering and Automobile
Universidad Antonio de Nebrija
C/ Pirineos 55, 28040 Madrid, Spain
e-mail: CMorenoRa@nebrija.es

Department of Mechanical Engineering and Aeronautics
City University of London
Northampton Square, EC1V 0HB London, United Kingdom
e-mail: Maria.Tomas-Rodriguez.1@city.ac.uk

† Electrical and Electronic Engineering Department
Imperial College London,
Exhibition Road, SW7 2AZ London, United Kingdom
e-mail: S.Evangelou@imperial.ac.uk

ABSTRACT

The effects of interconnected front and rear suspension systems on the in-plane dynamics of sport motorcycle is investigated. The interconnected suspension mathematical description is presented and included in a high-fidelity motorcycle model. The suspension behaviour under road step bump inputs is studied for different values of stiffness and damping interconnection coefficients. Optimal values of interconnection coefficients are proposed for the current motorcycle model. Finally, the oscillating dynamics of the motorcycle at straight running conditions is studied through its normal modes.

Keywords: motorcycle dynamics, suspension systems, interconnected suspensions, stability analysis.

1 INTRODUCTION

Interconnected suspensions have been widely used within the car industry. Nowadays most of the marketed cars are equipped with antiroll bars that connect mechanically the two wheels of the front and rear ends separately. Although the connection between the front and the rear ends is not as usual as the anti-roll bars, some notable example has been marketed, being the 1948 Citroën 2CV the first mass production car fitting this system. No many companies have published research on this topic, although some literature can be found. This is the case of Creuat [1] that published its research on semi-active/passive connected suspension system [6] from which the Hydropneumatic Suspension Systems LTT-Creuat has being developed [2]. However, in the two wheels field, these systems are not extended. Although some proposal can be found such is the case of the bicycle concept demonstrator developed by [7].

The interconnection of the front and rear suspension primarily affects the dynamics of the motorcycle on its symmetry plane. In the present research the effects of the interconnected suspensions on the in-plane motorcycle's dynamics are investigated. Firstly, the mathematical description of

an interconnected suspension system is developed (Section 2) to be included into a high-fidelity motorcycle model (Section 3). This model is used to carry out several simulations in which the motorcycle is forced to pass through a bump to obtain the response of the system (Section 4). An automatic optimization process is performed in order to obtain those values of the interconnection coefficients that better improve the suspension precision. The evolution of the eigenvalues and the eigenvectors corresponding to the in-plane normal modes are analysed (Section 5) to understand the effects of the interconnection arrangement on the oscillating dynamics of the motorcycle.

2 INTERCONNECTED SUSPENSION SYSTEM

In order to illustrate the interconnection concept in an intuitive manner, Figure 1 shows a sketch of an interconnected suspension system. In the actual motorcycle the front suspension system consists of a telescopic fork whilst the rear suspension system consists of a swinging arm reacting into the main frame. In order to follow this arrangement, a linear variable (z_f) is assigned to the front suspension compression whilst an angular variable (θ_r) is used for the rear suspension deflection.

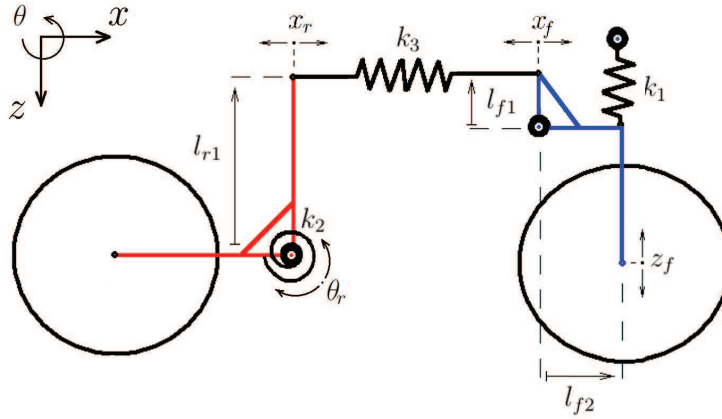


Figure 1: Diagram showing an schematic interconnection layout and its relevant parameters. The system can be divided in two rigid bodies, front (blue) and rear (red), connected through a spring-damper unit. In this figure only the springs are shown in order to provide a clearer view.

Considering small angles and linear approximations in Fig. 1, the stiffness reaction of the independent suspension systems are defined, on one hand, by Eq. 1 as a force applied to the front wheel depending linearly on its displacement with a stiffness constant k_1 . On the other hand, the reaction of the rear suspension is defined by Eq. 2 as a torque applied in the swinging arm depending linearly on its angular displacement with a rotational stiffness constant k_2 .

$$F_{1z} = -k_1 \cdot z_f \quad (1)$$

$$M_2 = -k_2 \cdot \theta_r \quad (2)$$

Once interconnection is considered, the total force and moment appearing on the front and rear suspension systems respectively become the addition of the independent force and moment and those equivalent force and moment due to the central spring (k_3): F_{3fz} and M_{3r} respectively.

$$F_{fk} = F_{1z} + F_{3fz} \quad (3)$$

$$M_{fk} = M_2 + M_{3r} \quad (4)$$

The resultant interconnection force and moment applied to the front and rear wheels respectively are obtained, through the geometrical ratios, from the force exerted by the central spring on its tips.

$$F_{3fz} = \rho_f \cdot F_{3fx} \quad (5)$$

$$M_{3r} = \rho_r \cdot F_{3rx} \quad (6)$$

The geometrical ratios will depend on the interconnection system's kinematics. For the sketch in Fig. 1 they can be defined considering small angles and the reference frame's sign criterion as follows:

$$\rho_f = -\frac{l_{f1}}{l_{f2}} \quad ; \quad \rho_r = l_{r1}$$

The forces exerted by the central spring depend on the relative displacements of its tips as follows:

$$F_{3fx} = -k_3 \cdot (x_f - x_r) \quad (7)$$

$$F_{3rx} = -k_3 \cdot (x_r - x_f) \quad (8)$$

The front (x_f) and the rear (x_r) displacements of the strut tips are related to the front wheel's vertical displacement and the swinging arm's rotation angle by the same geometrical ratios:

$$x_f = \rho_f \cdot z_f \quad ; \quad x_r = \rho_r \cdot \theta_r \quad (9)$$

Substituting in eq. 3 and eq. 4, the resultant front force and rear moment can be written as:

$$F_{fk} = -(k_1 + \rho_f^2 k_3) \cdot z_f + (\rho_f \rho_r k_3) \cdot \theta_r \quad (10)$$

$$M_{fk} = (\rho_f \rho_r k_3) \cdot z_f - (k_2 + \rho_r^2 k_3) \cdot \theta_r \quad (11)$$

A similar analysis can be done for the damping force and moment. If the geometric ratios for the damping system are named as μ_f and μ_r for the front and rear ends respectively, the resultant damping reactions can be written as:

$$F_{fc} = -(c_1 + \mu_f^2 c_3) \cdot \dot{z}_f + (\mu_f \mu_r c_3) \cdot \dot{\theta}_r \quad (12)$$

$$M_{fc} = (\mu_f \mu_r c_3) \cdot \dot{z}_f - (c_2 + \mu_r^2 c_3) \cdot \dot{\theta}_r \quad (13)$$

Finally, the resultant force and moment corresponding to the whole interconnected suspension system can be written as:

$$F_f = -k_f \cdot z_f - c_f \cdot \dot{z}_f - k_s \cdot \theta_r - c_s \cdot \dot{\theta} \quad (14)$$

$$M_r = -k_s \cdot z_f - c_s \cdot \dot{z}_f - k_r \cdot \theta_r - c_r \cdot \dot{\theta}_r \quad (15)$$

Within the interconnection approach, the total reaction force applied by the front telescopic fork is divided between the suspension and interconnection forces, which are defined independently. The front suspension force depends linearly on the front fork position and speed, whilst the front interconnection force does so on the rear swinging arm angle and rotational speed. For the rear end, the force is modelled in a similar way. In this case the rear suspension moment depends linearly on the swinging arm angle and rotational speed, whilst the rear interconnection moment does so on the front fork position and speed. Equations (14) and (15) show the total front suspension force and rear suspension moment.

Direct stiffness and damping equivalent coefficients (k_f , c_f , k_r and c_r) and cross stiffness and damping equivalent coefficient (k_s and c_s) are defined as:

$$k_f = k_1 + \rho_f^2 k_3 \quad ; \quad c_f = c_1 + \mu_f^2 c_3 \quad (16)$$

$$k_r = k_2 + \rho_r^2 k_3 \quad ; \quad c_r = c_2 + \mu_r^2 c_3 \quad (17)$$

$$k_s = -\rho_f \rho_r k_3 \quad ; \quad c_s = -\mu_f \mu_r c_3 \quad (18)$$

The units of the direct stiffness coefficients are Nm^{-1} and those of the direct damping coefficients are Nsm^{-1} . However, due to the geometrical ratio that convert forces into moments and vice versa, the units of the cross stiffness coefficients are N and those of the cross damping coefficients are Ns .

Note that the direct equivalent coefficients always take positive values whilst the cross equivalent coefficients can take either positive or negative values depending on the sign of the geometrical ratios. In Fig. 1, l_{f1} and l_{r1} are negative whilst l_{f2} is positive according to the sign criterion of the reference frame. Thus, ρ_f is positive and ρ_r is negative which results in $k_s > 0$. The cross coefficients represent the force/moment applied into the front/rear end due to the motion of the contrary end. For instance, a positive stiffness equivalent coefficient ($k_s > 0$) implies that a compression of the rear suspension system ($\theta < 0$), results in a force on the front suspension system that tries to extend it ($Z > 0$). Conversely, a negative stiffness coefficient ($k_s < 0$) would produce a force in the front suspension system that tries to compress it ($Z < 0$) when the rear end is compressed ($\theta < 0$).

3 SOFTWARE TOOLS AND MATHEMATICAL MODEL

The motorcycle model is implemented taking advantage of the VehicleSim multi-body software from Mechanical Simulation Corporation [8]. This suite consists of two separated tools: VS Lisp and VS Browser. VS Lisp is the tool used to generate the equations of motions from a multi-body description of any dynamical system. Making use of its own computer language (based on LISP) it is designed to automatically generate computationally efficient simulation programs for those multi-body systems. It can be configured to return either the corresponding non-linear equations of motion or the linearised equations of motion. Both non-linear and linearised equations of motion

are symbolically described as functions of all the parameters defining the model dynamics, such as suspensions or aerodynamics coefficients.

VS Browser is the front end of all the VehicleSim products. It provides a graphical context with a standard graphical user interface from which the non-linear equation of motion can be integrated using different built-in solvers. A compatibility Simulink module is provided by VehicleSim. This module can be included into the Simulink environment as a dynamical system that returns those outputs corresponding to the non-linear simulation carried out by VS Browser, which depend on the inputs introduced in it from the Simulink model. So that, external Matlab function (such as optimization ones) can iteratively run several dynamics simulations whilst motorcycle model's parameters are modified on-line.

On the other hand, the linearised equations of motion are returned in a Matlab file with the state space description of the systems. The state space matrices obtained (A, B, C and D) depend on both the system parameters and the state variables values. This feature becomes useful in the stability analysis of complex non linear systems, which can be linearised about operating points corresponding to quasi-equilibrium states. The frequency and damping coefficients associated to the system's normal modes are found through the eigenvalues of the state space matrix A.

The mathematical model used for this research is based on the model presented in [12]. This mathematical model was built during several years of research underpinned by wide literature and experimental data. This model has been extensively used in the past in numerous contributions such as , [5], [10], [4], [3] or [11].

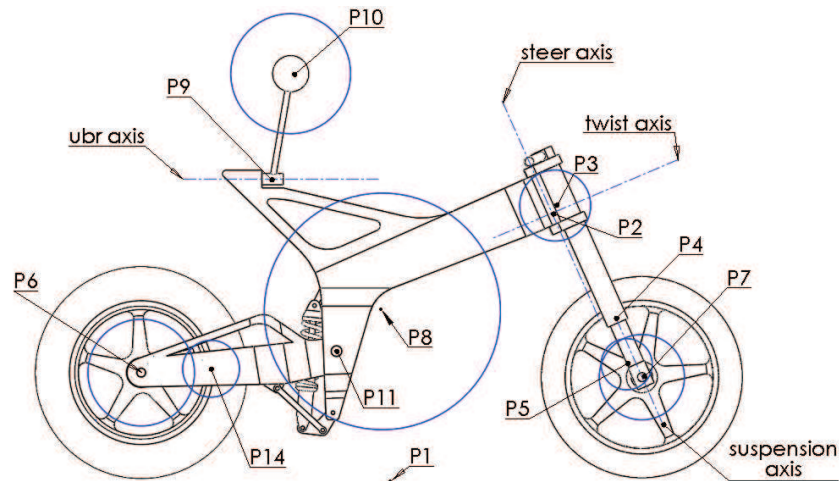


Figure 2: Motorcycle geometrical description. Blue circles with diameter proportional to body mass are plotted around the centre of mass of each body.

The model was developed using real dynamic parameters of an existing Suzuki GSX-R1000 K1. This machine is a good representative of contemporary commercial high performance motorcycles. It weights 170 kg and its in-line four cylinder and four stroke engine with 988 cc is able to deliver 160 hp.

The motorcycle model consists of seven bodies: rear wheel, swinging arm, main frame (comprising rider's lower body, engine and chassis), rider's upper-body, steering frame, telescopic fork suspension and front wheel. It involves 13 degrees of freedom: three rotational and three translational for the main frame, two rotational for the wheels spin, one rotational for the swinging arm, one rotational for the rider's upper body, one rotational for the frame flexibility, one rotational for the steering body and one translational for the front suspension fork. Figure 2 represents the main geometric points and axes in the motorcycle's geometry. The centre of mass of each of the seven

Table 1: Points defining the motorcycle geometry.

Point	Description
P1	Aerodynamic reference point.
P2	Twist body's joint with rear frame.
P3	Steer body's centre of mass.
P4	Front suspension body's joint with steer body.
P5	Front suspension body's centre of mass.
P6	Rear wheel's centre of mass and attachment point.
P7	Front wheel's centre of mass and attachment point.
P8	Main frame's centre of mass.
P9	Rider's Upper Body attachment point on rear frame
P10	Centre of mass of the rider's upper body.
P11	Swinging arm's attachment point on main frame.
P14	Swinging arm's centre of mass.

constituent bodies is represented as a blue circle with a diameter proportional to its mass. Table 1 contains the indexes of these points. For modelling purposes, a parent-child structure is used, as shown in Fig. 3.

The tires are treated as wide, flexible in compression and the migration of both contact points as the machine rolls, pitches and steers is tracked dynamically. The tyre's forces and moments are generated from the tyre's camber angle relative to the road, the normal load and the combined slip using Magic Formulae models [9]. This model is applicable to motorcycle tires operating at roll angles of up to 60° .

The aerodynamic drag/lift forces and pitching moment are modelled as forces/moments applied to the aerodynamic centre and they are proportional to the square of the motorcycle's forward speed. In order to maintain steady-state operating conditions, the model contains a number of control systems, which mimic the rider's control action. These systems control the throttle, the braking and braking distribution between the front and rear wheels, and the vehicle's steering.

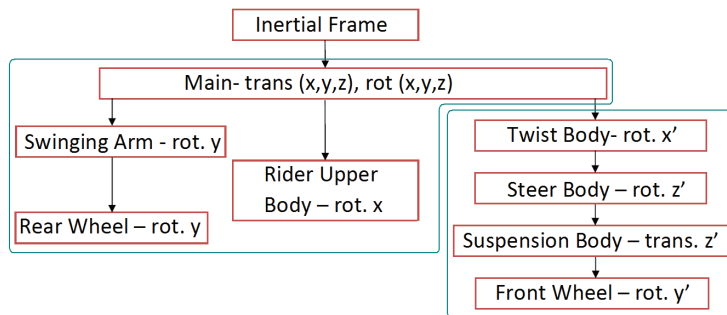


Figure 3: Parental structure of the motorcycle model.

The forward speed is maintained by a driving torque applied to the rear wheel and reacting on the main frame. This torque is derived from a proportional-integral (*PI*) controller on the speed error with fixed gains.

For some manoeuvres, the motorcycle is not self-stable; in order to stabilise the machine in such situations a roll angle feedback controller is implemented. This allows to obtain different steady turning equilibrium states which would not be stable without the roll angle controller. The con-

troller developed was a proportional-integral-derivative (*PID*) feedback of motorcycle lean angle error to steering torque. The lean angle target is set by an initial value and a constant change rate. Thus, the target lean angle is a ramp function of time which can be easily modified. The *PID* gains are defined as speed adaptive in order to achieve an effective stabilisation of the motorcycle for the difficult cases involving very low or very high speeds. Finally, the steering control torque is applied to the steer body reacting on the rider's upper body.

The front suspension system is defined as reacting force applied in the front fork's travel direction depending linearly on the compression of the fork. The rear suspension is described by a reacting torque on the swinging arm and which depends on its angular position to emulate the behaviour of the multi-lever rear suspension system of the actual motorcycle.

The scope of the present research is to study the effect of the interconnection itself on the motorcycle dynamics in comparison with the nominal suspension setting. For this reason, the nominal suspension forces and moments corresponding to the direct equivalent coefficients k_f , k_r , c_f and c_r are maintained unaffected in the model. Whilst the interconnection forces and moments are included, through the cross equivalent coefficients k_s and c_s , as additional terms to these nominal forces and moments. This means that the variation of the interconnection coefficient values will not affect the direct forces and moments.

4 ROAD BUMP INPUT RESPONSE

The main functions of a sport motorcycle suspension system are to provide enough precision for the wheels to follow the road profile as close as possible and to keep certain comfort levels for the rider under road perturbation. The non-linear model considered for this study introduces a discontinuity in the tires forces. As a result, these forces become zero when the tires take off from the road.

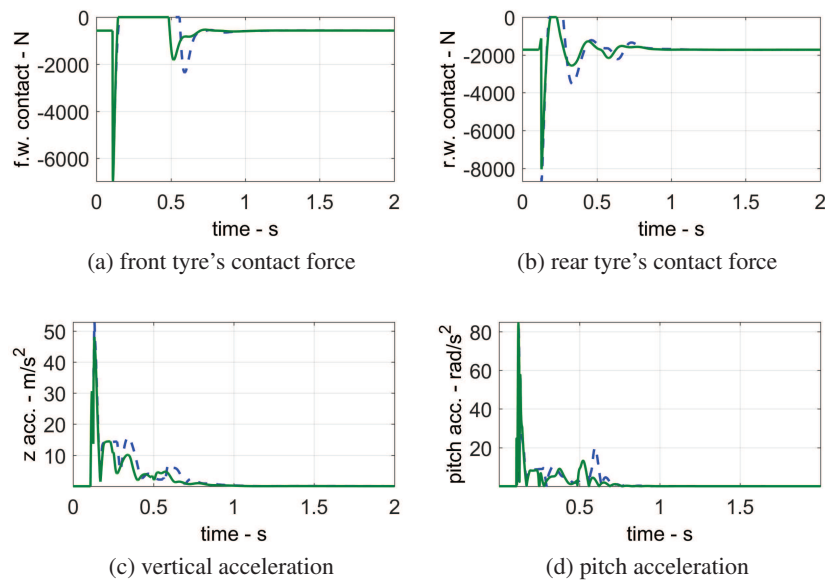


Figure 4: Precision and comfort variables responses at 80 m/s with interconnection coefficients $k_s = 0$ N and $c_s = -548$ Ns. The dashed blue line represents the nominal system response whilst the interconnected system response is plotted in solid green.

Wheels fly times (times during tyres loose contact with the road) have been considered as a mea-

surement for the suspension system's precision. Shorter fly times represent a greater precision. On the other hand, the comfort is measured through the maximum vertical acceleration and the maximum pitch angle acceleration perceived by the rider. Smaller values of these magnitudes for a bump input represent better comfort results.

The effect of the interconnection in the above mentioned variables is illustrated in Fig. 4. It shows the response of the motorcycle model to a step bump of height 0.05 m at a forward speed of 80 m/s. The interconnection coefficients are $k_s = 0$ N and $c_s = -548$ Ns. It can be observed how both front and rear wheels' fly times are reduced after the bump (Fig. 4a and Fig. 4b). The maximum vertical acceleration perceived by the rider is also reduced whilst the angular acceleration reaches similar values (Fig. 4c and Fig. 4d). The response of the independent suspension system in the nominal model is plotted in dashed blue line and the interconnected system's response is represented with a solid green line.

4.1 Suspension efficiency

In order to investigate the effects of the interconnection force and moment in the suspension response, the behaviours of these four variables are studied under straight forward bump simulations for a wide range of stiffness (k_s) and damping (c_s) interconnection coefficients. The focus of this study is to understand the effects that the interconnection introduces in the suspension's response. Therefore, the front and rear suspension coefficients are kept constant at their nominal values.

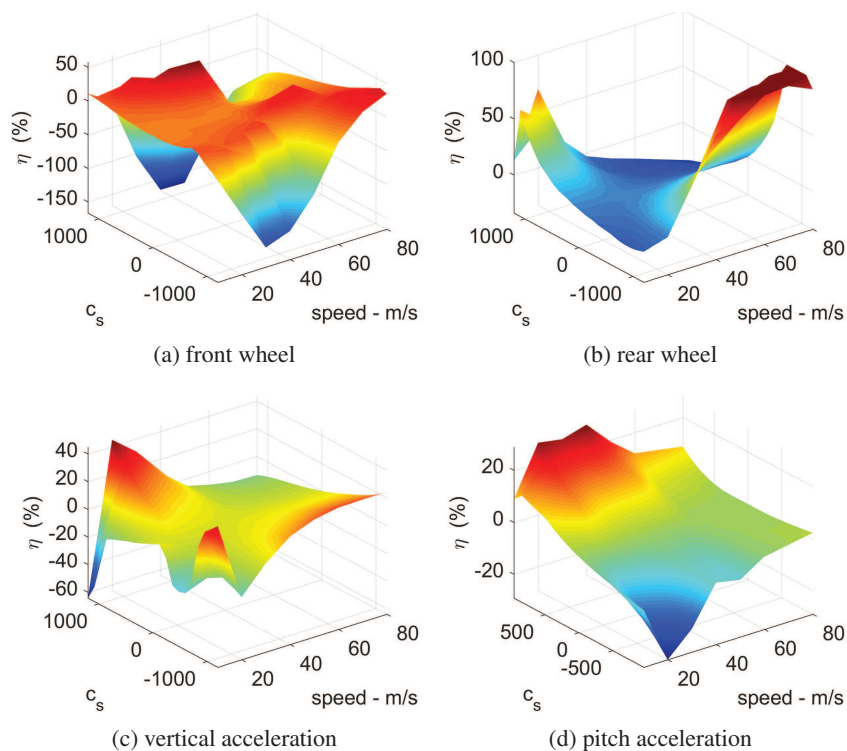


Figure 5: Efficiency maps of comfort and precision variables for different values of c_s with $k_s = 0$ N for a 0.05m step input at forward speeds starting at 10 m/s up to 80 m/s.

The suspension efficiency on each variable is defined as the normalized difference between the value achieved by the variable after a bump input with ($k_s \neq 0$ N or $c_s \neq 0$ Ns) and without

($k_s = 0$ N and $c_s = 0$ Ns) interconnection forces and moments. It is defined by the Eq. (19) as follows:

$$\eta(x) = 100 \cdot \frac{(x_0 - x)}{x_0} \quad (19)$$

Where x is the variable under study (it can be the maximum acceleration, the maximum pitch angle or the front/rear wheel fly times) and x_0 is the value achieved by the variable with independent suspensions. Efficiency is expressed as a percentage and it will be positive if the connection set-up provides a reduction on the variable's value.

Eight simulation scenarios have been created in VS Browser corresponding to eight forward speeds starting at 10 m/s and reaching 80 m/s. In these simulations the motorcycle is forced to pass through a road bump of 0.05 m at a constant speed. These scenarios are called from a Simulink model from where the stiffness and damping values are taken. The Simulink model is placed in a loop where these coefficients are varied sequentially, performing all the simulations for values of k_s ranging from -12000 N to 12000 N and values of c_s ranging from -1200 Ns to 1200 Ns. Figure 5 shows the results of varying the interconnection damping coefficient (c_s) and the speed, whilst the interconnection stiffness coefficient is $k_s = 0$ N. In Fig. 6 the interconnection damping coefficient is kept constant at zero ($c_s = 0$ Ns) whilst the values of the interconnection stiffness coefficient k_s and the forward speed are varied.

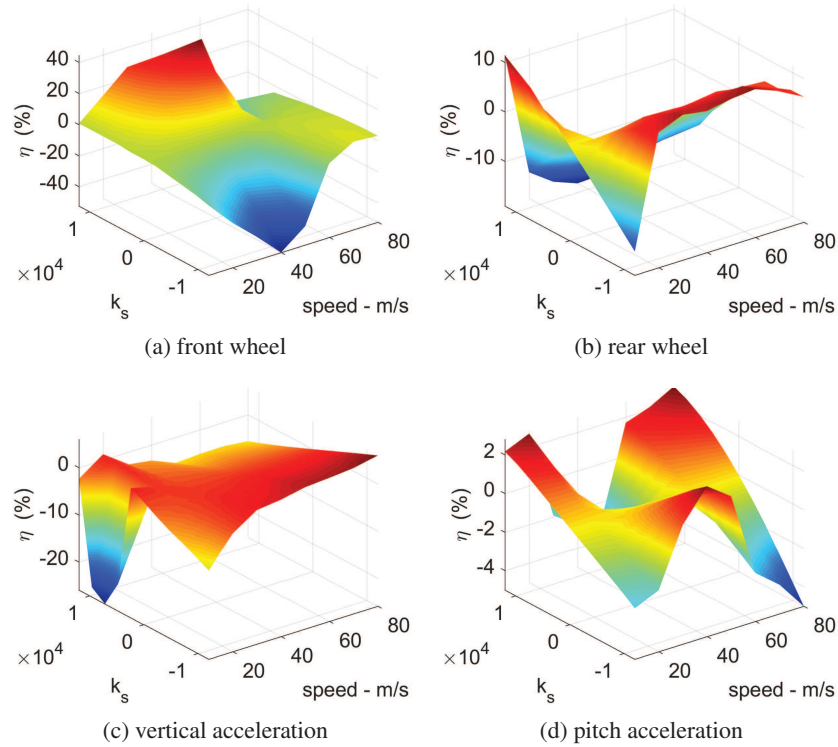


Figure 6: Efficiency maps of comfort and precision variables for different values of k_s with $c_s = 0$ Ns for a 0.05 m step input at forward speeds starting at 10 m/s up to 80 m/s.

The combination of stiffness and damping coefficients in the interconnected suspension system makes difficult to find those coefficients that could improve the efficiency of the variables under

study simultaneously. However, an automatic optimization processes can be implemented in order to find these optimal coefficients.

4.2 Optimization of the stiffness and damping coefficients

Two optimal values of the interconnection parameters k_s and c_s are sought for the full speed range. Considering that the model under study corresponds to a high performance racing motorcycle, the optimization process is now focused in obtaining a greater suspension precision.

For each of the eight considered forward speeds, the target function to be maximized is defined as the front wheel fly time efficiency. This is, to minimize the front wheel's fly time. Matlab optimization toolbox is a good framework to find satisfying results within a reasonable computational time. The optimization process takes advantage of 'fminsearch' function which is feed with the corresponding target function. The target function calls sequentially eight Simulink models that contain the different VehicleSim Blocks for the eight forward speeds under study. The sum of all the efficiencies is established as the function's target to be maximized.

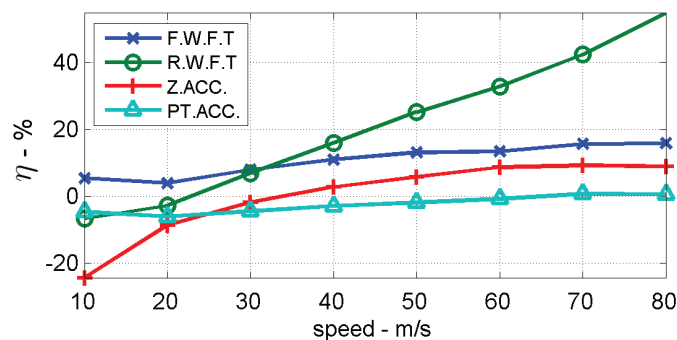


Figure 7: Efficiencies of the precision and comfort variables obtained for the optimal interconnection parameters' values.

The optimal configuration found for the speed range is $k_s \approx 0$ N and $c_s = -548$ Ns. The results of the optimization processes are presented in Fig. 7. The efficiencies on the front wheel (*FW*), rear wheel (*RW*), vertical acceleration (*ACC*) and pitch angle acceleration (*PTC*) are shown for the entire speed range. The improvement percentage of the suspension response of the front wheel starts around 5 % at low speeds and rises up to 17 % at high speeds. The rear suspension response is improved for high speeds and slightly worsened for very low speeds, but its efficiency never decays below the -7 %. Considering that the front wheel is relevant in terms of rider's control and that the rear wheel fly time is only increased for very low speeds, this can be considered a good result for a simple interconnection system. Although the optimization processes have not taken the comfort into account, it is not worsened in a substantial manner and, in some cases, it is improved.

5 OSCILLATING DYNAMICS

As it has been previously explained, VehicleSim returns a state space representation of the programmed model. This is an automatically generated Matlab file containing the state matrices A, B, C and D. The terms of these matrices are expressed as functions of the state variables (positions and velocities) as well as the different dynamical parameters of the motorcycle model (masses, inertias, etc.). The parameters are numerically set in the Matlab file according to the values defined in the model programmed in VS-Lisp, in contrast to the state variables that are free to be set depending on the trim state to be studied.

In order to study the evolution of the normal modes with respect to the speed variation, several simulations are run. On each simulation, the speed is increased from 10 m/s up to 80 m/s with a very low ratio (0.001 m/s^2) in order to obtain quasi-equilibrium trim states. Once a simulation is finished, the values of the state variables for each forward speed are taken from those of the corresponding simulation time step. The state matrices are then fed with these values, resulting in a high fidelity state space representation for each trim state and from which its normal modes can be obtained.

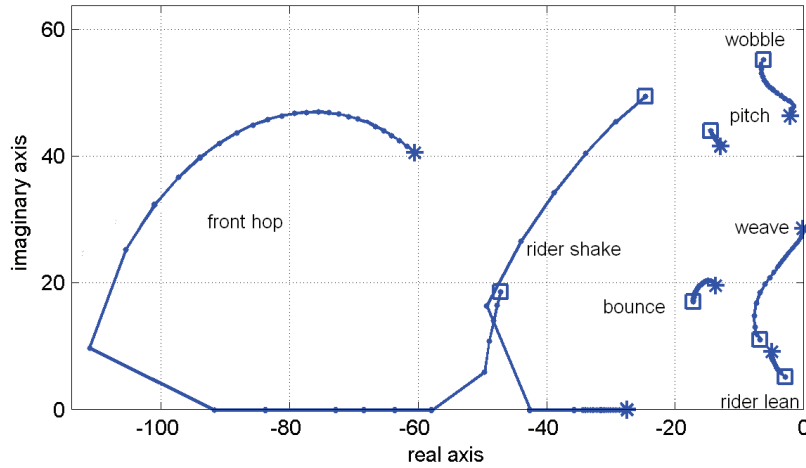


Figure 8: Root loci for the motorcycle nominal suspension system showing the main normal modes affected by the suspension dynamics. Speed is increased from 10 m/s (□) up to 80 m/s (*) in straight running conditions.

The eigenvalues of the state space matrix A provide information on the normal modes' frequency and damping for a given trim state and can be represented as a root locus. Figure 8 shows a root locus for the motorcycle nominal configuration in which no connection exists between the front and rear suspension systems, for speed ranging from 10 m/s (□) up to 80 m/s (*) in straight running conditions.

Table 2: Eigenvectors' components of the motorcycle multi-body system.

DOF	Description
XT, YT, ZT	Motorcycle's chassis x , y and z translation.
ZR, YR, XR	Motorcycle's chassis yaw , $pitch$ and $roll$ rotations.
SWA	Swinging arm rotation about the main frame's y axis.
UBR	Rider's upper-body rotation about the main frame x axis.
TWS	Front frame rotation about the $twist$ axis.
STR	Front frame rotation about the $steering$ axis.
SUS	Front fork compression/extension.

This root locus shows a wide area where highly damped normal modes are visible. Clearly, these modes do not imply stability risks for the motorcycle nominal configuration. They hardly could be excited and, thus, appreciated in the motorcycle dynamics. However, once the front and rear suspension systems are connected, these modes change its damping properties in a substantial manner approaching the unstable region.

The normal modes shown in this plot are divided into in-plane and out-of-plane modes. The in-plane modes are those in which only the degrees of freedom that imply a motion inside the

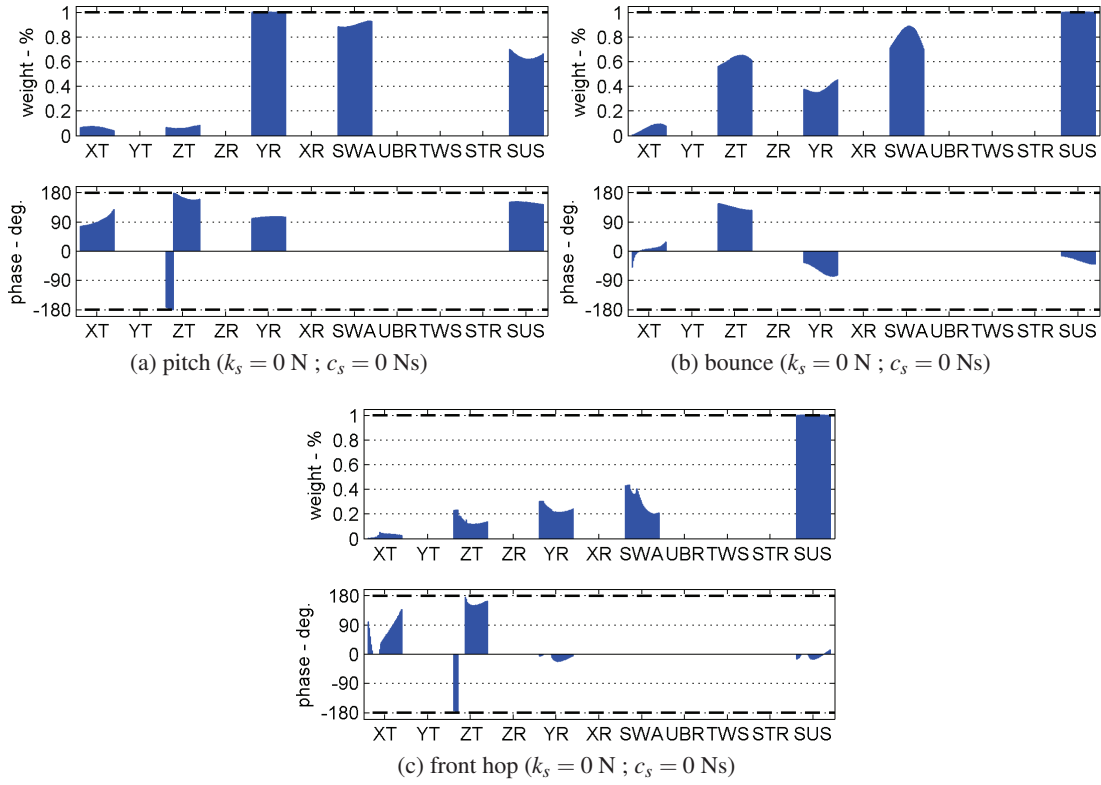


Figure 9: In-plane normal modes' components at straight running conditions for the motorcycle nominal configuration. The speed evolution of each component's weight and phase is represented by the bars profile, varying the speed from left (10 m/s) to right hand side (80 m/s).

motorcycle's symmetry plane are involved. They are pitch, bounce and front hop. On the other hand, the out-of-plane modes only involve the degrees of freedom that represent a motion out of the motorcycle's symmetry plane. The out-of-plane modes are wobble, weave, rider lean and rider shake.

The interconnected suspension system mostly affects the in-plane dynamics of the motorcycle. Thus, it has a higher impact on in-plane normal modes. In order to understand its effects on the pattern of motion of these normal modes, the weights and the phase angles of the different degrees of freedom involved in such modes are obtained from the components of the eigenvectors of the state space matrix A associated to them. In this paper, normal modes are represented by two bar diagrams. In the first of them, the bars heights represent normalized weights of the normal mode's degrees of freedom. In the second diagram, the bars heights represent the relative phase angle of each degree of freedom. The degrees of freedom in the x coordinates of the normal mode figures are all related to the motorcycle's reference frame and they are presented in Table 2.

The eigenvector of the in-plane modes for the nominal model without interconnected suspensions are presented in Fig. 9. The pitch mode's components are shown in Fig. 9a. They are characterized by the main body pitching (YR) with large oscillations of the front (SUS) and rear (SWA) suspension. The phase angle presented by the pitching of the motorcycle's main frame with respect to the front suspension and the swinging arm is close to -90° and 90° respectively. For a motorcycle model with a perfect symmetry about its centre of masses there would not be other components involved and the phase angle between the front suspension and the rear swinging arm would be

exactly 180° , producing a pure pitch motion. However, this model presents differences in terms of masses, suspensions, etc. of the front and rear sides of the motorcycle, these other components such as the vertical (ZT) or the horizontal (XT) displacements are present in the mode motion, and the phase angles are smaller than 180° . This normal mode is well damped and its frequencies are constricted between 40 rad/s and 45 rad/s.

The components of the bounce mode are plotted in Fig. 9b. It consists in the vertical oscillation of the main frame (ZT) almost in phase opposition with the front (SUS) and rear (SWA) suspensions. Similarly than what happens with pitch mode, other degrees of freedom are involved on the bounce mode which presents these phase angles smaller than 180° . Once again, this is due to the model asymmetry around its centre of masses. For a symmetrical model, this mode would present a pure bounce motion pattern. It is also well damped and its frequencies are in the range of 15 rad/s to 20 rad/s.

The front hop mode corresponds to the front wheel resonance whilst the rest of motorcycle assembly remains slightly affected. Figure 9c shows how the main component of its eigenvector is the front suspension (SUS) oscillation with minor lower oscillation of the rest of the in-plane degrees of freedom. For this motorcycle model, and with no interconnection established between front and rear suspensions, it is a highly damped mode with a large frequency variation with the speed. It can reach values up to 45 rad/s at medium-high speeds and becomes overcritical for low-medium speed range.

In previous section was found that the optimal value of the interconnection stiffness coefficient is very close to $k_s = 0$ and that for the interconnection damping coefficient is $c_s = -548$ Ns. In order to understand the effect of these optimal values on the normal modes, the eigenvalues and eigenvectors of matrix A are calculated with these values. Also, c_s is varied from 0 Ns up to -1500 Ns to observe the evolution of the normal modes in terms of natural frequency and damping ratio introduced by this kind of negative interconnection. Figure 10 represents the evolution of the motorcycle's root locus when the interconnection damping coefficients are varied within these limits.

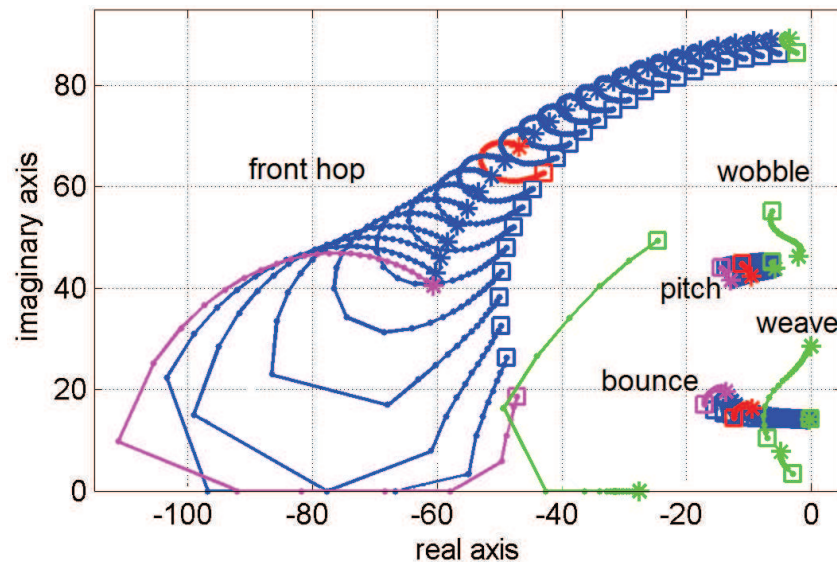


Figure 10: Root loci showing the main normal modes evolution for values of the interconnection damping coefficient ranging from $c_s = -1500$ Ns (magenta) to $c_s = 0$ Ns (green). The root locus for the optimal interconnection damping coefficient $c_s = -548$ Ns is plotted in red. Speed is increased from 10 m/s (\square) up to 80 m/s ($*$).

The optimal configuration is plotted in red. As expected, out-of-plane modes remain unaffected. On the other hand, pitch, bounce and front hop damping ratio are reduced although they stay stable for this configuration. However, if the negative interconnection coefficient is increased in absolute value all the three modes get much closer to the positive area of the real axis, thus, to the stability limit. The normal mode which is affected the most is the front hop. In order to observe possible variation on their pattern of motion Fig. 11 shows the eigenvector components of these modes.

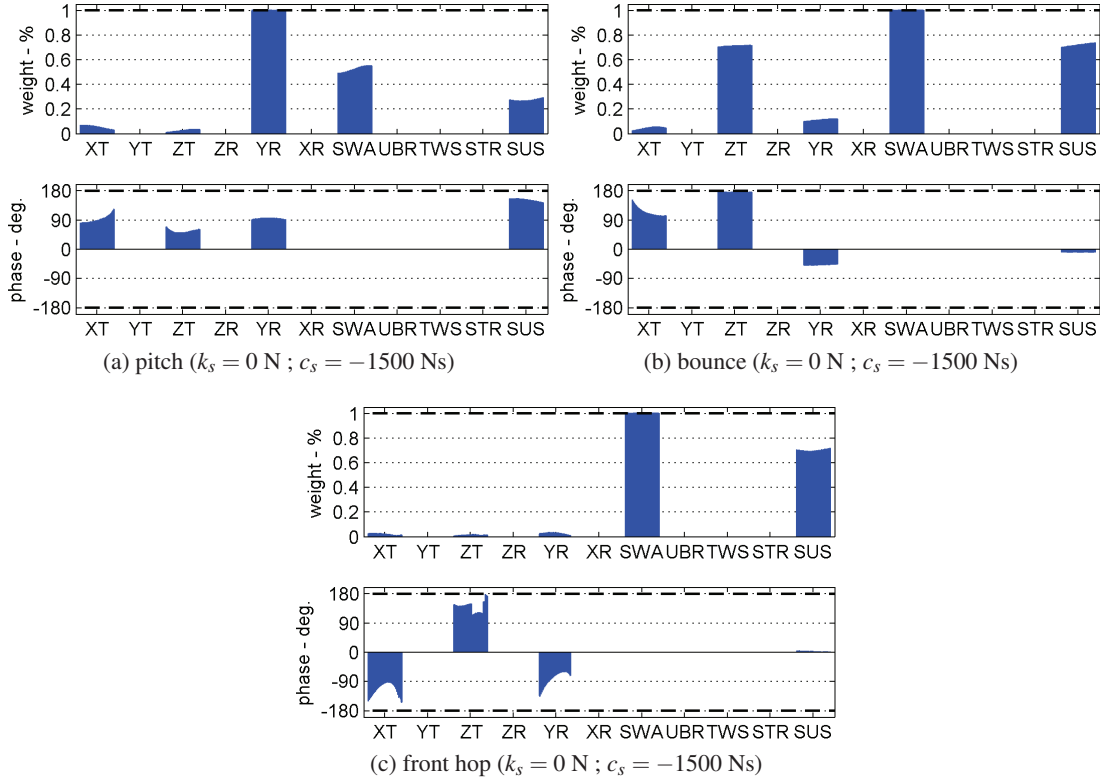


Figure 11: In-plane normal modes' components at straight running conditions for an interconnection damping coefficient of $c_s = -1500 \text{ Ns}$. The speed evolution of each component's weight and phase is represented by the bars profile, varying the speed from left (10 m/s) to right hand side (80 m/s).

For the bounce and pitch normal mode, their pattern of motion remain recognizable. Although small changes on the phases of some of their less relevant degrees of freedom appear, the most significant variations are observed in their main degrees of freedom.

On one hand, for the pitch mode, those degrees of freedom associated to the suspension motion (SUS and SWA) decrease their relative weights with respect to the main degree of freedom for this mode, the pitch rotation (YR).

On the other hand, the opposite happens for the bounce mode. The degrees of freedom associated to the suspension motion (SUS and SWA) increase their relative weights with respect to the vertical displacement (ZT) which is the main degree of freedom for this mode.

However, the pattern of motion related to the front hop mode has drastically changed. For the nominal configuration ($c_s = 06 \text{ Ns}$) the main degree of freedom was the front suspension (SUS). Nevertheless, as the interconnection negative damping coefficient is increased (in absolute value), the relative weight of this degree of freedom is reduced whilst the degree of freedom associated to

the rear suspension (SWA) increases its weight taking higher relevance than the front suspension degree of freedom.

Once the interconnection is set between the front and the rear suspension systems, there exists a transfer of energy between these two systems that modifies their behaviour. As it has been stated before, negative interconnection coefficients imply that a compression of one of the two systems will result in a force that tries to compress the other one and vice versa. This fact is consistent with what it is observed in the evolution of the patterns of motion of the in-plane normal modes. Firstly, in the front hop mode, the interconnection increases the rear suspension (SWA) motion whilst keeps the phase of both front and rear suspension degrees of freedom close to zero. Secondly, such interconnection favours the front (SUS) and rear (SWA) suspension motion (which are in phase) in the bounce mode with respect to the vertical displacement (ZT). Whilst in the case of the pitch mode, the interconnection penalizes those suspension motions (which are in phase opposition) with respect to the pitch rotation (YR).

6 CONCLUSIONS AND FURTHER WORK

This research presents the potential benefits in terms of performance that an interconnected suspensions system could introduce in a motorcycle, if adequately implemented.

For the motorcycle model under study, it has been shown that satisfactory results are achieved in terms of tyre fly time reduction by the connection of the front and rear suspension, just by means of a simple damper unit. After an optimization process which looks for improve the suspension precision in a wide speed range, it has been found that negative values of interconnection damping coefficients are suitable whilst interconnection stiffness coefficients can be neglected.

Nevertheless, the study of the eigenvalues and eigenvectors related to the in-plane normal modes predicts a destabilization and an increase of the frequency of some modes that, in the nominal configuration (without interconnection), are very well damped. This is the case of the front hop mode. Further more, this mode also changes its pattern of motion increasing drastically the rear suspension oscillation when high values of interconnection damping coefficient are set.

Further research on the effect of interconnected suspension coefficients on the motorcycle's dynamics and oscillating modes is being carried out in order to obtain a wider view on the overall impact of including an interconnected suspension on sport motorcycles. The present research is being extended to study the effects of negative and positive interconnection coefficients, not only on the motorcycle in-plane dynamics but also on the out-of-plane dynamics, considering the impact of the interconnection on both the in-plane and out-of-plane normal modes when the motorcycle is leaning at different roll angles.

REFERENCES

- [1] Creuat. **url:** <http://www.creuat.com>. Accessed: 2017-11-07.
- [2] Hydropneumatic suspension systems LTT-Creuat. **url:** <http://www.lleidatracciotechnology.com/productos.php>. Accessed: 2018-10-20.
- [3] EVANGELOU, S., LIMEBEER, D., AND TOMAS-RODRIGUEZ, M. Suppression of burst oscillations in racing motorcycles. In 2010 49th IEEE Conference on Decision and Control (CDC) (2010), pp. 5578–5585.

- [4] EVANGELOU, S., LIMEBEER, D. J., AND TOMAS RODRIGUEZ, M. Influence of road camber on motorcycle stability. Journal of Applied Mechanics 75, 6 (2008), pp. 061020–061020.
- [5] EVANGELOU, S., LIMEBEER, D. J. N., SHARP, R. S., AND SMITH, M. C. Mechanical steering compensators for high-performance motorcycles. Journal of Applied Mechanics 74, 2 (2006), pp. 332–346.
- [6] FONTDECABA I BUJ, J. Integral suspension system for motor vehicles based on passive components. SAE Technical Paper 2002-01-3105, SAE International, 2002.
- [7] GRIFFITHS, A. The Toptrail interconnected suspension bicycle project.
url: www.toptrail.co.uk. Accessed: 2018-10-20.
- [8] MECHANICAL SIMULATION CORPORATION. Vehiclesim technology.
url: www.carsim.com. Accessed: 2018-10-20.
- [9] PACEJKA, H. B., AND BAKKER, E. The magic formula tyre model. Vehicle System Dynamics 21 (1992), pp. 1–18.
- [10] SHARP, R. S. Motorcycle steering control by road preview. Journal of Dynamic Systems, Measurement, and Control 129, 4 (2007), pp. 373–382.
- [11] SHARP, R. S. Rider control of a motorcycle near to its cornering limits. Vehicle System Dynamics 50, 8 (2012), pp. 1–16.
- [12] SHARP, R. S., EVANGELOU, S., AND LIMEBEER, D. J. N. Advances in the modelling of motorcycle dynamics. Multibody System Dynamics 12, 3 (2004), pp. 251–283.